

Light vector mediators facing XENON1T data

D. Aristizabal Sierra,^{1,2,*} V. De Romeri,^{3,†} L. J. Flores,^{4,‡} and D. K. Papoulias^{5,§}

¹Universidad Técnica Federico Santa María - Departamento de Física
Casilla 110-V, Avda. España 1680, Valparaíso, Chile

²IFPA, Dep. AGO, Université de Liège, Bat B5, Sart Tilman B-4000 Liège 1, Belgium

³Institut de Física Corpuscular CSIC/Universitat de València, Parc Científic de Paterna
C/ Catedrático José Beltrán, 2 E-46980 Paterna (Valencia) - Spain

⁴Instituto de Física, Universidad Nacional Autónoma de México, A.P. 20-364, Ciudad de México 01000, México.

⁵Department of Physics, University of Ioannina GR-45110 Ioannina, Greece

Recently the XENON1T collaboration has released new results on searches for new physics in low-energy electronic recoils. The data shows an excess over background in the low-energy tail, particularly pronounced at about 2 – 3 keV. With an exposure of 0.65 tonne-year, large detection efficiency and energy resolution, the detector is sensitive as well to solar neutrino backgrounds, with the most prominent contribution given by pp neutrinos. We investigate whether such signal can be explained in terms of new neutrino interactions with leptons mediated by a light vector particle. We find that the excess is consistent with this interpretation for vector masses below $\lesssim 0.1$ MeV. The region of parameter space probed by the XENON1T data is competitive with constraints from laboratory experiments, in particular GEMMA, Borexino and TEXONO. However we point out a severe tension with astrophysical bounds and cosmological observations.

I. INTRODUCTION

Dark matter (DM) direct detection experiments have entered the era of ton-size active volumes, and will keep going in that direction in their search for DM signals [1–5]. Combined with high sensitivities at low energy thresholds as well as low and fairly well-understood backgrounds, these experiments offer opportunities in the search for DM signals which cover large classes of DM physics models. Conventional searches using nuclear recoil energy measurements allow searches of DM in the GeV–TeV range, while electron recoil measurements provide a tool for sub-GeV DM and other well-motivated degrees of freedom such as axion-like particles (ALPs) and/or dark photons [6, 7]. Being sensitive to irreducible solar neutrino backgrounds, they will enable as well a better understanding of solar neutrino fluxes [8, 9] and potentially new directions in the search for new physics in the neutrino sector [10–13].

XENON1T is a dual-phase liquid xenon time projection chamber with a one-tonne active target [1]. The detector conceived for WIMP DM searches in regions above ~ 6 GeV can be used as well for searches of ALPs, dark photons and neutrino properties, thanks to the low energy thresholds and background rates. Given its dual-phase character, prompt scintillation and delayed luminescence signals— $S1$ and $S2$ —can be well measured. Identification of electron and nuclear recoils can be done through $S2/S1$ ratios, and thus provide a tool for particle identification (e.g. neutron-induced nuclear recoils from β -induced electron recoils). Recently XENON1T has released data taken from February 2017 to February 2018, in which signals above background-induced electron recoil

events were searched for [14]. The collaboration has reported an excess below 7 keV with a prominent feature towards 2 – 3 keV. Using this data, three new physics scenarios were explored as possible explanations to the signal: the solar axion model, neutrino magnetic moment and bosonic dark matter. The finding shows that the resulting 90% CL parameter space regions within which the excess can be accounted for are disfavored by astrophysical arguments [15–17]. The collaboration has as well tested this result against possible background from tritium β decays. In this case the statistical significance of the new physics hypotheses is substantially diminished.

Although the background hypothesis cannot be discarded, one can as well entertain the possibility that the excess is driven by new physics. Indeed, seemingly, this has been the approach the collaboration has adopted. If one is to adopt such approach as well, there is a lesson one should take from the findings the collaboration has reported: *Whatever the nature of the new physics is, it should be able to produce localized spectral distortions.* Above 7 keV the data is rather well described by the background, e.g. in the range 25 – 50 keV the data points are beautifully accounted for by the radio activity of ^{83m}Kr [14].

Possible scenarios of new physics are those in which electron recoils are modified by the coupling of new degrees of freedom to electrons. The new degrees of freedom could e.g. involve DM or particles from a dark sector [18–22]. Another possibility, which goes along the lines of the neutrino magnetic moment, is an interaction that locally enhances the elastic scattering neutrino-electron cross section [23]. That is actually what the neutrino magnetic moment does, it adds to the electroweak neutral and charged current neutrino-electron cross section, dominating the scattering process at low recoil energies. Possibilities include neutrino non-standard interactions (NSI) as well as neutrino generalized interactions (NGI) [24–28], both with electrons. In the effective limit— $m_{\text{Med}}^2 \gg q^2$ (q being the exchanged momentum)—these interactions will produce overall enhancements or depletions (de-

* daristizabal@ulg.ac.be

† deromeri@ific.uv.es

‡ luisjf89@fisica.unam.mx

§ d.papoulias@uoi.gr

pletions only if the new interaction is driven by vector boson exchange) of the SM expectation. Thus, given the typical exchanged momentum, spectral distortions can be generated only by light mediators, of which in this paper we consider the vector case.

The paper is organized as follows. In Sec. II we discuss the relevant interactions, the neutrino-electron differential cross section and the neutrino backgrounds at XENON1T. In Sec. III we present our results: the event rates, the phenomenological constraints on light vector states and a statistical analysis of the parameter space. We summarize in Sec. IV.

II. LIGHT VECTOR MEDIATOR SCENARIOS AND SOLAR NEUTRINO BACKGROUND

The interactions that we consider can be understood as a consequence of a larger complete theory that we do not specify. They could be e.g. the result of an extended gauge group U_{B-L} or $U(1)_X$ [29, 30]. For the purpose of this paper what matters is the presence of a new light vector mediator, coupled to neutrinos and electrons, although one could in principle include the other charged leptons too. Along the same lines one could as well consider a kinetic mixing term, between the hypercharge field of the SM and the new vector. For simplicity—however—we set the tree level coupling to zero, bearing in mind that it then will be generated radiatively and hence it will be suppressed.

The elastic neutrino-electron cross section involves the SM charged- and neutral-current contributions as well as a new neutral-current piece induced by the light vector. The cross section has been calculated in several papers [10, 24, 30–32]. Here we use the expression derived in Ref. [30] which applies in $U(1)_X$ models in which neutrino and electron charges Q_X are dictated by anomaly cancellation conditions. It reads

$$\frac{d\sigma}{dE_r} = \frac{m_e G_F^2}{4\pi} \left[g_2^2 + g_1^2 \left(1 - \frac{E_r}{E_\nu} \right)^2 - g_1 g_2 \frac{m_e E_r}{E_\nu^2} \right], \quad (1)$$

where the couplings $g_{1,2}$ include both the SM and new physics components as follows

$$g_{1,2} = g_{1,2}^{\text{SM}} + a_{1,2} + \frac{b_{1,2}}{G_F(2m_e E_r + m_V^2)}. \quad (2)$$

In the expression above, G_F stands for the Fermi coupling constant, E_r refers to the electron recoil energy, E_ν denotes the incoming neutrino energy, m_e is the electron mass and m_V the mass of the new vector mediator. In the limit of suppressed mass mixing between the neutral vectors, the SM pieces are given by their standard forms in terms of the weak-mixing angle s_W^2 , as

$$g_1^{\text{SM}} = -2\sqrt{2}s_W^2, \quad g_2^{\text{SM}} = \sqrt{2}(1 - 2s_W^2) - 2\sqrt{2}, \quad (3)$$

with the second term in g_2^{SM} being present only for electron neutrinos. The SM limit is then given by

$$\frac{d\sigma_{\text{SM}}}{dE_r} = \frac{d\sigma}{dE_r} \Big|_{a_i=b_i=0}. \quad (4)$$

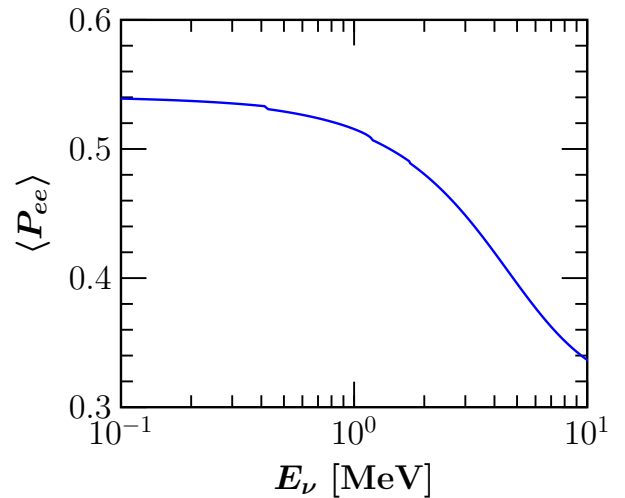


FIG. 1. Averaged survival probability $\langle P_{ee} \rangle$ versus neutrino energy calculated in the two-flavor approximation with neutrino production distribution functions and neutrino fluxes (pp and CNO) as given in the BS05 Standard Solar Model [33]. We have fixed the neutrino oscillation parameters according to their best fit point values [34].

Full expressions for the a_i and b_i parameters are given in Ref. [30]. In the limits assumed in this paper (suppressed kinetic and mass mixing), they have a rather simple form

$$a_1 = a_2 = 0, \quad b_1 = -\frac{1}{4} Q_V^L Q_\ell^R g_V^2, \quad b_2 = -\frac{1}{4} Q_V^L Q_\ell^L g_V^2, \quad (5)$$

where g_V is the coupling associated to the new vector boson and possible charge choices are determined by anomaly cancellation, as in Ref. [29]. Out of the possible choices, $Q_V^L = Q_\ell^R = Q_\ell^L = -1$ corresponds to the well known U_{B-L} case. In the following we stick to this scenario. From Eq. (2), one can see that a spectral feature in the electron recoil events can be generated by the $q^2 = -2m_e E_r$ dependence, as far as the vector is not decoupled. This is the limit we are interested in.

Having introduced the notation, we then move on to the determination of the *morphology* of the neutrino background at XENON1T. With a 0.65 tonne-year exposure, the expected number of solar neutrino electron recoil events is 220.7 ± 6.6 [14]. This background can be obtained by integrating the following differential rate [12]

$$\frac{dR}{dE_r} = \epsilon N_T \sum_\alpha \int_{E_\nu^{\min}}^{E_\nu^{\max}} \frac{d\Phi_\alpha}{dE_\nu} \left[P_{ee} \frac{d\sigma_e}{dE_r} + (1 - P_{ee}) \frac{d\sigma_f}{dE_r} \right] dE_\nu, \quad (6)$$

with α running over all the neutrino-related subprocesses of the solar pp and CNO chains: pp , ${}^8\text{B}$, hep , two ${}^7\text{Be}$ and pep lines, ${}^{13}\text{N}$, ${}^{15}\text{O}$ and ${}^{17}\text{F}$. Here ϵ refers to the exposure in tonne-year, $N_T = (Z_{\text{Xe}}/m_{\text{molar}})N_A$ to the number of target electrons per tonne of material and $d\Phi_\alpha/dE_\nu$ to neutrino flux in $\text{cm}^{-2}\text{year}^{-1}\text{MeV}^{-1}$ units. For the solar neutrino fluxes we take the predictions of the BS05 Standard Solar Model [33].

Expression (6) assumes the two-flavor approximation, a fairly accurate limit given that $\Delta m_{12}^2/\Delta m_{13}^2 \ll 1$. In this limit

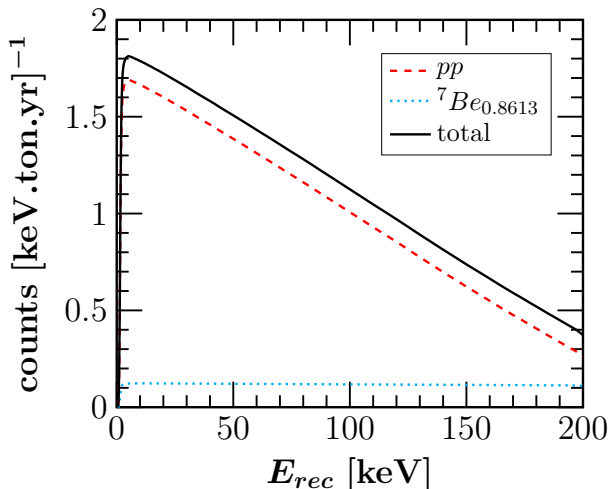


FIG. 2. Expected number of neutrino-electron scattering events per tonne-year-keV induced by solar neutrinos. Most events are generated by the continuous pp flux. E_{rec} refers to reconstructed energy, see Sec. III for details.

one neutrino eigenstate is mainly ν_e with flavor contamination suppressed by the reactor mixing angle, while the other—labeled f —is a superposition of ν_μ and ν_τ with the admixture determined by the atmospheric mixing angle. The survival probability proceeds from an average over the neutrino trajectory and weighted by solar neutrino production distributions determined by the BS05 Standard Solar Model. For its calculation we have proceeded as described in Refs. [12, 35]. Figure 1 shows our result derived for neutrino oscillation parameters fixed according to the best fit point value obtained from global neutrino oscillation data analysis: $\Delta m_{12}^2 = 7.55 \times 10^{-5} \text{ eV}^2$, $\sin^2 \theta_{12} = 0.32$ and $\sin^2 \theta_{13} = 0.0216$ [34].

The differential cross section in the first term of Eq. (6) is given by Eq. (4), the one in the second term as well but without including the second term in g_2^{SM} in Eq. (3). The lower integration limit is related to the recoil energy through

$$E_\nu^{\text{min}} = \frac{1}{2} \left(E_r + \sqrt{E_r^2 + 2E_r m_e} \right), \quad (7)$$

while for E_ν^{max} we take the kinematic end points of each of the neutrino fluxes. Although the sum in (6) covers all neutrino emission processes, given the recoil window, we find that the pp continuous spectrum alone accounts for almost all the solar neutrino background. This is somehow expected given the low energy threshold achieved by the detector, 1 keV, and the size of the different components of the neutrino flux. Figure 2 shows the differential event rate calculated with Eq. (6). There one can see that pp neutrinos dominate the signal all over E_r . Other contributions are subdominant, including the ${}^7\text{Be}$ line at 0.861 MeV (the second relevant contribution) and ${}^8\text{B}$ which for CEvNS will be the dominant source [36].

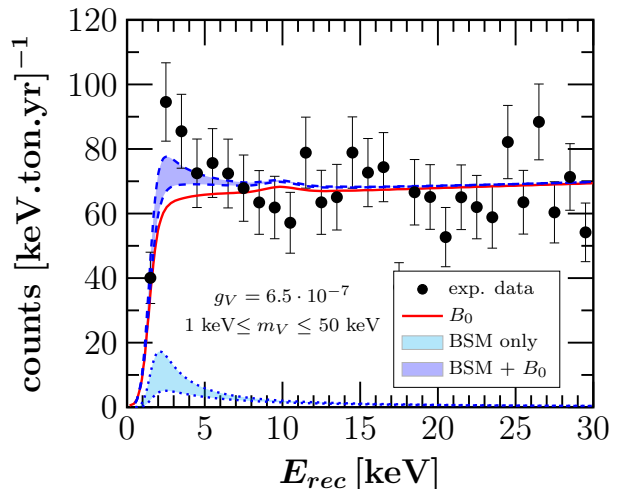


FIG. 3. XENON1T data points along with the predicted background (B_0). The peaked signals at low energies are generated by a light vector mediator coupled to both electron-neutrinos and electrons and so contributing to the elastic scattering neutrino-electron cross section. The signals are generated using the benchmark points $m_V \in [1, 50] \text{ keV}$ and $g_V = 6.5 \times 10^{-7}$. E_{rec} refers to reconstructed energy, see Sec. III for details.

III. CONSTRAINTS AND PARAMETER SPACE ANALYSIS

In what follows we assume that only ν_e couples to the light new vector boson while ν_f is subject only to SM couplings. Including coupling to ν_f will not change our conclusions qualitatively. Although the new interaction can affect neutrino propagation in matter, here it is reasonable to consider only effects in detection. Forward coherent scattering is responsible for matter effects, which given the solar electron density are prominent (resonantly enhanced) only for ${}^8\text{B}$ neutrinos. Since the signal is driven by the pp flux, propagation effects can be safely ignored. Under those well-justified assumptions, the second term in Eq. (6) is negligible. However, for completeness, we keep the full expression in our calculation.

Figure 3 shows the effect of the new interaction on the neutrino-electron differential event rate, along with the data points of XENON1T and the background B_0 , assuming a fixed value of g_V and scanning over m_V in the range $[1, 50] \text{ keV}$ (width of the light blue band). The signal peaks at low energies with decreasing vector boson masses, for fixed coupling. This behavior is expected from the structure of the differential cross section. The third term in Eq. (2) has a recoil energy dependence, which becomes irrelevant for sufficiently large m_V . However, in the limit $2m_e E_r \gg m_V^2$ that term behaves like $\sim E_r^{-1}$. Therefore, in that regime, the E_r dependence is basically the same of the $\nu - e$ neutrino magnetic moment cross section [37–39].

To statistically determine the regions favored/disfavored by XENON1T data we define a simple spectral χ^2 function as

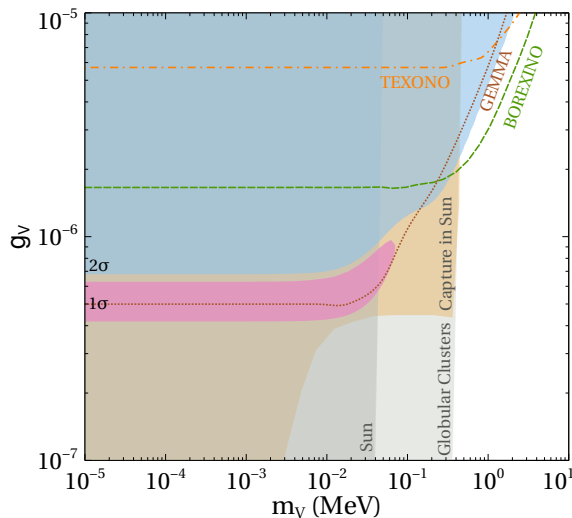


FIG. 4. Allowed 1σ and excluded 2σ regions in the $m_V - g_V$ plane for light vector mediators. Along with the regions, laboratory limits from TEXONO [42], GEMMA [43, 44] and Borexino [45, 46] as well as those from astrophysics [47–51] are shown as well.

follows

$$\chi^2 = \sum_{a=1}^{29} \frac{1}{\sigma_a^2} \left[\left(\frac{dR^{V+B_0}}{dE_{\text{rec}}} \right)_a - \left(\frac{dR^{\text{Exp}}}{dE_{\text{rec}}} \right)_a \right]^2. \quad (8)$$

Here σ_a refers to statistical uncertainty per bin, E_{rec} to reconstructed recoil energy and B_0 to background. To compare with the experimental results from XENON1T we have convolved the differential rate given in Eq. (6) with a normalized Gaussian function with an energy-dependent standard deviation defined as: $\sigma/E_{\text{rec}} = a/\sqrt{E_{\text{rec}}} + b$, $a = (31.71 \pm 0.65)\% \text{keV}^{1/2}$, $b = (0.15 \pm 0.02)\%$ [40, 41]. We further apply the detector efficiency [14], after the smearing. dR/E_{rec} in Eq. (8) refers to the quantity obtained that way. Note that given that the shift between the nominal and reconstructed energies is always below 0.4% [41], differences between results with or without smearing are minor.

Following XENON1T analysis, we have added B_0 to the vector contribution. The allowed 1σ region (pink) and 2σ excluded region (light blue region) resulting from our analysis are shown in Fig. 4. At the 1σ level, the allowed vector boson masses are always below ~ 800 keV with couplings that never exceed 6×10^{-7} . In this region the largest enhancements in the $2 - 7$ keV energy range are found. As m_V increases, the E_r^{-1} behavior of the cross section diminishes and the differential recoil spectrum flattens out towards B_0 .

At this point then the question is whether the 1σ allowed region is consistent with existing bounds on light vector mediator scenarios, for example those in [10, 30, 50–52] (some of them relevant also for CEvNS [53, 54]). These bounds can be separated in laboratory, astrophysical and cosmological constraints. In the region of interest, the most stringent laboratory limits are set by TEXONO, GEMMA and Borexino [42–46], as shown in Fig. 4. XENON1T improves the constraints on light vector mediators for $m_V \lesssim 0.2$ MeV, compared to TEX-

ONO and Borexino. GEMMA limits are tighter but still leave unconstrained a fraction of the 1σ region. Overall, the regions within which XENON1T excess can be accounted for are consistent with laboratory bounds.

Astrophysical and cosmological constraints are instead much more severe. The light vectors can be produced in environments like horizontal branch stars and the Sun leading then to energy losses [47–49, 55]. The presence of a vector neutrino coupling can affect the neutrino mean free path in supernovae, eventually disrupting the neutrino diffusion time [56]. These arguments lead to stringent bounds within the region of interest (see Fig. 4). In general, these limits might be evaded if the vector boson couples to light scalars that undergo condensation in the corresponding environment. Under these conditions the vector mass becomes environmental dependent and so its production is no longer possible [57]. Further relevant bounds come from cosmology. In the early Universe the vector boson can thermalize through neutrino or electron annihilation or scattering processes. This will alter the expansion history of the early Universe and eventually lead to a sizeable contribution to the effective number of neutrino species, ΔN_{eff} [58–62]. While the exact evaluation of these bounds will depend on the specific model and thermal history of the Universe, they appear to exclude the full XENON1T 1σ -region here derived.

IV. CONCLUSIONS

We have considered light vector mediator scenarios in the light of the recent XENON1T data [14]. We have addressed the question of whether these interactions can account for the spectral distortion observed by the collaboration. Light vector mediators generate spectral features, modifying the recoil energy dependence of the differential cross section, which increases at low E_r for sufficiently small vector boson masses. We have performed a statistical analysis taking into account the complete set of solar neutrino fluxes and the neutrino survival probability from oscillations. We have shown that XENON1T bounds are competitive with those from other laboratory experiments. Astrophysical and cosmological observations place instead more severe constraints, which potentially exclude the regions of parameter space which can explain the XENON1T excess. With increasing exposures, multi-ton LXe detectors will keep on testing other parameter space regions of these scenarios.

Note added in proof

While completing this work, Ref. [23] appeared in the arXiv database. In addition to light vector mediators, this paper considered as well light scalar mediators. Our findings are consistent with those this reference has reported.

ACKNOWLEDGMENTS

DAS is supported by the grant “Unraveling new physics in the high-intensity and high-energy frontiers”, Fondecyt No 1171136. VDR acknowledges financial support by the SEJI/2018/033 grant, funded by Generalitat Valenciana and partial support by the Spanish grants FPA2017-90566-REDC (Red Consolider MultiDark), FPA2017-85216-P and PROM-

ETEO/2018/165 (Generalitat Valenciana). LJF is supported by a postdoctoral CONACYT grant. The work of DKP is co-financed by Greece and the European Union (European Social Fund- ESF) through the Operational Programme “Human Resources Development, Education and Lifelong Learning” in the context of the project “Reinforcement of Postdoctoral Researchers - 2nd Cycle” (MIS-5033021), implemented by the State Scholarships Foundation (IKY).

-
- [1] E. Aprile et al. (XENON), *JCAP* **1604**, 027 (2016), 1512.07501.
- [2] J. Aalbers et al. (DARWIN), *JCAP* **1611**, 017 (2016), 1606.07001.
- [3] C. E. Aalseth et al., *Eur. Phys. J. Plus* **133**, 131 (2018), 1707.08145.
- [4] D. S. Akerib et al. (LUX-ZEPLIN) (2018), 1802.06039.
- [5] M. Schumann, L. Baudis, L. Btikofer, A. Kish, and M. Selvi, *JCAP* **1510**, 016 (2015), 1506.08309.
- [6] L. Di Luzio, M. Giannotti, E. Nardi, and L. Visinelli (2020), 2003.01100.
- [7] R. Essig et al., in *Community Summer Study 2013: Snowmass on the Mississippi* (2013), 1311.0029.
- [8] J. L. Newstead, L. E. Strigari, and R. F. Lang (2018), 1807.07169.
- [9] J. L. Newstead, R. F. Lang, and L. E. Strigari (2020), 2002.08566.
- [10] D. G. Cerdeño, M. Fairbairn, T. Jubb, P. A. N. Machado, A. C. Vincent, and C. Boehm, *JHEP* **05**, 118 (2016), [Erratum: *JHEP*09,048(2016)], 1604.01025.
- [11] B. Dutta, S. Liao, L. E. Strigari, and J. W. Walker, *Phys. Lett.* **B773**, 242 (2017), 1705.00661.
- [12] D. Aristizabal Sierra, N. Rojas, and M. H. G. Tytgat, *JHEP* **03**, 197 (2018), 1712.09667.
- [13] M. C. Gonzalez-Garcia, M. Maltoni, Y. F. Perez-Gonzalez, and R. Zukanovich Funchal, *JHEP* **07**, 019 (2018), 1803.03650.
- [14] E. Aprile et al. (XENON) (2020), 2006.09721.
- [15] S. A. Daz, K.-P. Schrder, K. Zuber, D. Jack, and E. E. B. Barrios (2019), 1910.10568.
- [16] M. Giannotti, I. G. Irastorza, J. Redondo, A. Ringwald, and K. Saikawa, *JCAP* **10**, 010 (2017), 1708.02111.
- [17] A. H. Crsico, L. G. Althaus, M. M. Miller Bertolami, S. Kepler, and E. Garca-Berro, *JCAP* **08**, 054 (2014), 1406.6034.
- [18] F. Takahashi, M. Yamada, and W. Yin (2020), 2006.10035.
- [19] K. Kannike, M. Raidal, H. Veerme, A. Strumia, and D. Teresi (2020), 2006.10735.
- [20] G. Alonso-Ivarez, F. Ertas, J. Jaeckel, F. Kahlhoefer, and L. Thormaehlen (2020), 2006.11243.
- [21] B. Fornal, P. Sandick, J. Shu, M. Su, and Y. Zhao (2020), 2006.11264.
- [22] J. Smirnov and J. F. Beacom (2020), 2002.04038.
- [23] C. Boehm, D. G. Cerdeno, M. Fairbairn, P. A. Machado, and A. C. Vincent (2020), 2006.11250.
- [24] A. Bolanos, O. G. Miranda, A. Palazzo, M. A. Tortola, and J. W. F. Valle, *Phys. Rev.* **D79**, 113012 (2009), 0812.4417.
- [25] Y. Farzan and M. Tortola (2017), 1710.09360.
- [26] P. Coloma, I. Esteban, M. C. Gonzalez-Garcia, and M. Maltoni (2019), 1911.09109.
- [27] D. Aristizabal Sierra, V. De Romeri, and N. Rojas, *Phys. Rev.* **D98**, 075018 (2018), 1806.07424.
- [28] A. N. Khan, W. Rodejohann, and X.-J. Xu (2019), 1906.12102.
- [29] M. D. Campos, D. Cogollo, M. Lindner, T. Melo, F. S. Queiroz, and W. Rodejohann, *JHEP* **08**, 092 (2017), 1705.05388.
- [30] M. Lindner, F. S. Queiroz, W. Rodejohann, and X.-J. Xu, *JHEP* **05**, 098 (2018), 1803.00060.
- [31] P. Ballett, M. Hostert, S. Pascoli, Y. F. Perez-Gonzalez, Z. Tabrizi, and R. Zukanovich Funchal, *Phys. Rev. D* **100**, 055012 (2019), 1902.08579.
- [32] J. B. Dent, B. Dutta, S. Liao, J. L. Newstead, L. E. Strigari, and J. W. Walker, *Phys. Rev. D* **96**, 095007 (2017), 1612.06350.
- [33] J. N. Bahcall, A. M. Serenelli, and S. Basu, *Astrophys. J.* **621**, L85 (2005), astro-ph/0412440.
- [34] P. F. de Salas, D. V. Forero, C. A. Ternes, M. Tortola, and J. W. F. Valle, *Phys. Lett.* **B782**, 633 (2018), 1708.01186.
- [35] M. C. Gonzalez-Garcia and M. Maltoni, *JHEP* **09**, 152 (2013), 1307.3092.
- [36] L. E. Strigari, *New J. Phys.* **11**, 105011 (2009), 0903.3630.
- [37] P. Vogel and J. Engel, *Phys. Rev.* **D39**, 3378 (1989).
- [38] N. F. Bell, M. Gorchtein, M. J. Ramsey-Musolf, P. Vogel, and P. Wang, *Phys. Lett. B* **642**, 377 (2006), hep-ph/0606248.
- [39] N. F. Bell, V. Cirigliano, M. J. Ramsey-Musolf, P. Vogel, and M. B. Wise, *Phys. Rev. Lett.* **95**, 151802 (2005), hep-ph/0504134.
- [40] E. Aprile et al. (XENON), *Nature* **568**, 532 (2019), 1904.11002.
- [41] E. Aprile et al. (XENON) (2020), 2003.03825.
- [42] M. Deniz et al. (TEXONO), *Phys. Rev. D* **81**, 072001 (2010), 0911.1597.
- [43] A. Beda, E. Demidova, A. Starostin, V. Brudanin, V. Egorov, D. Medvedev, M. Shirchenko, and T. Vylov, *Phys. Part. Nucl. Lett.* **7**, 406 (2010), 0906.1926.
- [44] A. Beda, V. Brudanin, V. Egorov, D. Medvedev, V. Pogosov, M. Shirchenko, and A. Starostin (2010), 1005.2736.
- [45] M. Agostini et al. (BOREXINO), *Nature* **562**, 505 (2018).
- [46] G. Bellini et al., *Phys. Rev. Lett.* **107**, 141302 (2011), 1104.1816.
- [47] J. A. Grifols and E. Masso, *Phys. Lett.* **B173**, 237 (1986).
- [48] J. A. Grifols, E. Masso, and S. Peris, *Mod. Phys. Lett.* **A4**, 311 (1989).
- [49] J. H. Chang, R. Essig, and S. D. McDermott, *JHEP* **09**, 051 (2018), 1803.00993.
- [50] R. Harnik, J. Kopp, and P. A. N. Machado, *JCAP* **1207**, 026 (2012), 1202.6073.
- [51] S. Bilmis, I. Turan, T. M. Aliev, M. Deniz, L. Singh, and H. T. Wong, *Phys. Rev.* **D92**, 033009 (2015), 1502.07763.
- [52] M. Bauer, P. Foldenauer, and J. Jaeckel, *JHEP* **07**, 094 (2018), 1803.05466.
- [53] D. Aristizabal Sierra, V. De Romeri, and N. Rojas, *JHEP* **09**, 069 (2019), 1906.01156.
- [54] D. Aristizabal Sierra, B. Dutta, S. Liao, and L. E. Strigari, *JHEP* **12**, 124 (2019), 1910.12437.
- [55] J. B. Dent, F. Ferrer, and L. M. Krauss (2012), 1201.2683.

- [56] J. H. Chang, R. Essig, and S. D. McDermott, *JHEP* **01**, 107 (2017), 1611.03864.
- [57] A. E. Nelson and J. Walsh, *Phys. Rev.* **D77**, 095006 (2008), 0802.0762.
- [58] E. Masso and R. Toldra, *Phys. Lett. B* **333**, 132 (1994), hep-ph/9404339.
- [59] B. Ahlgren, T. Ohlsson, and S. Zhou, *Phys. Rev. Lett.* **111**, 199001 (2013), 1309.0991.
- [60] A. Kamada, K. Kaneta, K. Yanagi, and H.-B. Yu, *JHEP* **06**, 117 (2018), 1805.00651.
- [61] M. Escudero, D. Hooper, G. Krnjaic, and M. Pierre, *JHEP* **03**, 071 (2019), 1901.02010.
- [62] B. Dutta, S. Ghosh, and J. Kumar (2020), 2002.01137.